9th International Conference on Clifford Algebras
and their Applications in Mathematical Physics
K. Gürlebeck (ed.)
Weimar, Germany, 15–20 July 2011

COLOR EXTENSION OF MONOGENIC WAVELETS WITH GEOMETRIC ALGEBRA : APPLICATION TO COLOR IMAGE DENOISING

R. Soulard* **and P. Carré**

**Xlim-SIC laboratory*
University of Poitiers, France
E-mail: raphael.soulard@univ-poitiers.fr

Keywords: Color Wavelets, Analytic, Monogenic, Wavelet transforms, Image analysis, Denoising.

Abstract. *We define a color monogenic wavelet transform. This is based on the recent grayscale monogenic wavelet transform and an extension to color signals aimed at defining non-marginal tools. Wavelet based color image processing schemes have mostly been made by using a grayscale tool separately on color channels. This may have some unexpected effect on colors because those marginal schemes are not necessarily justified. Here we propose a definition that considers a color (vector) image right at the beginning of the mathematical definition so we can expect to bring an actual color wavelet transform - which has not been done so far to our knowledge. This so provides a promising multiresolution color geometric analysis of images. We show an application of this transform with a statistical modeling of coefficients for color denoising issue.*

1 INTRODUCTION

Wavelets have been widely used for handling images for more than 20 years. It seems that the human visual system sees images through different channels related to particular frequency bands and directions; and wavelets provide such decompositions. Since 2001, the *analytic signal* and its 2D generalizations have brought a great improvement to wavelets [1, 2, 3] by a natural embedding of an AM/FM analysis in the subband coding framework. This yields an efficient representation of geometric structures in grayscale images thanks to a *local phase* carrying geometric information complementary to an *amplitude envelope* having good invariance properties. So it codes the signal in a more coherent way than standard wavelets. The last and seemingly most appropriate proposition [3] of *analytic wavelets* for image analysis is based on the *monogenic signal* [4] defined with geometric algebra.

In parallel a *color monogenic signal* was proposed [5] as a mathematical extension of the monogenic signal; paving the way to non-marginal color tools especially by using geometric algebra and above all by considering a color signal right at the foundation of the mathematical construction.

We define here a *color monogenic wavelet transform* that extends the monogenic wavelets of [3] to color. These *analytic wavelets* are defined for color 2D signals (images) and avoid the classical pitfall of marginal processing (grayscale tool used separately on color channels) by relying on a sound mathematical definition. We may so expect to handle coherent information of multiresolution color geometric structure; which would make easier any wavelet based color image processing. To our knowledge color wavelets have not been proposed so far.

We first give a technical study of analytic signal/wavelets with the intent to popularize them since they rely on non-trivial concepts of geometric algebra, complex/harmonic analysis, as well as non-separable wavelet frames. Then we describe our *color monogenic wavelet transform*; and finally an application to color denoising will be presented.

Notations :
2-vector coordinates : $\boldsymbol{x}=(x,y)$, $\boldsymbol{\omega}=(\omega_1,\omega_2) \in \mathbb{R}^2$; $\boldsymbol{k} \in \mathbb{Z}^2$
Euclidean norm : $\|\boldsymbol{x}\| = \sqrt{x^2+y^2}$
Complex imaginary number : $\boldsymbol{j} \in \mathbb{C}$ Argument of a complex number : $\arg$
Convolution symbol : $*$ Fourier transform : $\mathcal{F}$

2 ANALYTIC SIGNAL AND 2D GENERALIZATION

An *analytic signal* s_A is a multi-component signal associated to a real signal s to analyze. The definition is well known in the 1D case where $s_A(t) = s(t) + \boldsymbol{j}\ (h * s)(t)$ is the complex signal made of s and its Hilbert transform (with $h(t) = \frac{1}{\pi t}$).

The polar form of the 1D analytic signal provides an AM/FM representation of s with $|s_A|$ being the *amplitude envelope* and $\varphi = \arg(s_A)$ the *instantaneous phase*. This classical tool can be found in many signal processing books and is used in communications for example.

Interestingly we can also interpret the phase in terms of signal shape *i.e.* there is a direct link between the angle φ and the *local structure* of s. Such a link between a 2D phase and local geometric structures of images would be very attractive in image processing. That is why there were several attempts to generalize it for 2D signals; and among them the *monogenic signal* [4] seems the most advanced since it is rotation invariant.

The Monogenic Signal

Without going beyond strictly needed details we here review the key points of the fundamental construction of the monogenic signal; which will be necessary to understand the color extension.

The definition of the 1D case given above can be interpreted in terms of *signal processing* : the Hilbert transform makes a "pure $\frac{\pi}{2}$-dephasing". But such a dephasing is not straightforward to define in 2D (same issue with many 1D signal tools) so let us look at the equivalent *complex analysis* definition of the 1D analytic signal. It says that s_A is the *holomorphic extension* of s restricted to the real line. But complex algebra is impeding for generalizations to higher dimensions. To bypass this limitation we can see a *holomorphic function* like a 2D *harmonic field* that is an equivalent *harmonic analysis* concept involving the 2D Laplace equation $\Delta f = 0$. It so can be generalized within the framework of 3D harmonic fields by using the 3D Laplace operator $\Delta_3 = \left(\frac{\delta}{\delta x} + \frac{\delta}{\delta y} + \frac{\delta}{\delta z}\right)$. The whole generalization relies on this natural choice and remaining points are analogous to the 1D case (see [4] for more details). Note that in Felsberg's thesis this construction is expressed in terms of *geometric algebra* but here we avoided it for simplicity's sake. Finally the 2D monogenic signal s_A associated to s is the 3-vector valued signal :

$$s_A(\boldsymbol{x}) = \begin{bmatrix} s(\boldsymbol{x}) \\ s_{r1}(\boldsymbol{x}) = \frac{x}{2\pi\|\boldsymbol{x}\|^3} * s(\boldsymbol{x}) \\ s_{r2}(\boldsymbol{x}) = \frac{y}{2\pi\|\boldsymbol{x}\|^3} * s(\boldsymbol{x}) \end{bmatrix} \tag{1}$$

Where s_{r1} and s_{r2} are analogous to the imaginary part of the complex 1D analytic signal. Interestingly, this construction reveals the two components of a Riesz transform :

$$\mathcal{R}\{s\} = (\ s_{r1}(\boldsymbol{x})\ ,\ s_{r2}(\boldsymbol{x})\ ) = \left(\ \frac{x}{2\pi\|\boldsymbol{x}\|^3} * s(\boldsymbol{x})\ ,\ \frac{y}{2\pi\|\boldsymbol{x}\|^3} * s(\boldsymbol{x})\ \right) \tag{2}$$

in the same way that the 1D case exhibits a Hilbert transform. Note that we get back to a *signal processing* interpretation since the Riesz transform can also be viewed like a pure 2D dephasing. In the end, by focusing on the *complex analysis* definition of the analytic signal we end up with a convincing generalization of the Hilbert transform.

Now recall that the motivation to build 2D analytic signals arises from the strong link existing between the phase and the geometric structure. To define the 2D phase related to the Riesz transform the actual monogenic signal must be expressed in spherical coordinates that yield the following amplitude envelope and 2-angle phase :

$$\begin{array}{ll|l} \text{Amplitude :} & A = \sqrt{s^2 + s_{r1}^2 + s_{r2}^2} & s = A\cos\varphi \\ \text{Orientation :} & \theta = \arg\left(s_{r1} + \boldsymbol{j}\ s_{r2}\right) & s_{r1} = A\sin\varphi\cos\theta \\ \text{1D Phase :} & \varphi = \arccos\left(\frac{s}{A}\right) & s_{r2} = A\sin\varphi\sin\theta \end{array} \tag{3}$$

Felsberg shows a direct link between the angles θ and φ and the geometric local structure of s. The signal is so expressed like an "A-strong" 1D structure with orientation θ. φ is analogous to the 1D local phase and indicates if the structure is rather a line or an edge. A direct drawback is that intrinsically 2D structures are not handled. Yet this tool found many applications in image analysis from contour detection to motion estimation (see [3] and references therein p. 1).

From a *signal processing* viewpoint the AM/FM representation provided by an analytic signal is accordingly well suited for narrowband signals. That is why it seems natural to embed it in a wavelet transform that performs subband decomposition. We now present the monogenic wavelet analysis proposed in [3].

3 MONOGENIC WAVELETS

So far there is one proposition of computable monogenic wavelets in the literature [3]. It provides 3-vector valued monogenic subbands consisting of a rotation-covariant *magnitude* and this new 2D *phase*. This representation - specially defined for 2D signals - is a great theoretic improvement of the complex and quaternion wavelets [1, 2]; as well as the monogenic signal itself is an improvement of its complex and quaternion counterparts.

The proposition of [3] consists of one real-valued "primary" wavelet transform in parallel with an associated complex-valued wavelet transform. Both transforms are linked each other by the Riesz transform so they carry out a multiresolution monogenic analysis. We end up with 3-vector coefficients forming subbands that are monogenic.

3.1 Primary transform

The primary transform is real-valued and relies on a dyadic pyramid decomposition tied to a wavelet frame. Only one 2D wavelet is needed and the dyadic downsampling is done only at the low frequency branch; leading to a redundancy of 4:3. The scaling function φ_γ and mother wavelet ψ are defined in the Fourier domain :

$$\varphi_\gamma \overset{\mathcal{F}}{\longleftrightarrow} \frac{\left(4(\sin^2\frac{\omega_1}{2}+\sin^2\frac{\omega_2}{2})-\frac{8}{3}\sin^2\frac{\omega_1}{2}\sin^2\frac{\omega_2}{2}\right)^{\frac{\gamma}{2}}}{\|\boldsymbol{\omega}\|^\gamma} \tag{4}$$

$$\psi(\boldsymbol{x}) = (-\Delta)^{\frac{\gamma}{2}}\ \varphi_{2\gamma}(2\boldsymbol{x}) \tag{5}$$

Note that φ_γ is a cardinal polyharmonic spline of order γ and spans the space of those splines with its integer shifts. It also generates - as a scaling function - a valid multiresolution analysis.

This particular construction is made by an extension of a wavelet basis (non-redundant) related to a critically-sampled filterbank. This extension to a wavelet frame (redundant) adds some degrees of freedom used by the authors to tune the involved functions. In addition a specific *subband regression* algorithm is used at the synthesis side. The construction is fully described in [6].

3.2 The monogenic transform

The second "Riesz part" transform is a complex-valued extension of the primary one. We define the associated complex-valued wavelet by including the Riesz components :

$$\psi' = -\left(\frac{x}{2\pi\|\boldsymbol{x}\|^3} * \psi(\boldsymbol{x})\right) + \boldsymbol{j}\left(\frac{y}{2\pi\|\boldsymbol{x}\|^3} * \psi(\boldsymbol{x})\right) \tag{6}$$

It can be shown that it generates a valid wavelet basis and that it can be extended to the pyramid described above. The joint consideration of both transforms form monogenic subbands from which can be extracted the amplitude and phase for an overall redundancy of 4:1.

So far no applications of the monogenic wavelets have been proposed. In [3] a demonstration of AM/FM analysis is done with fine orientation estimation and gives very good results in terms of coherency and accuracy. Accordingly this tool may be rather used for analysis tasks than processing.

Motivated by the powerful analysis provided by the monogenic wavelet transform we propose now to extend it for color images.

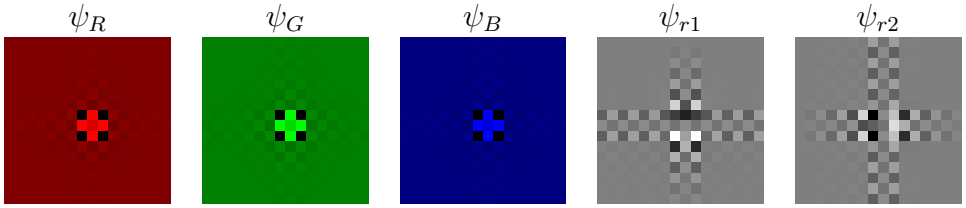

Figure 1: Space representation of the 5 color wavelets.

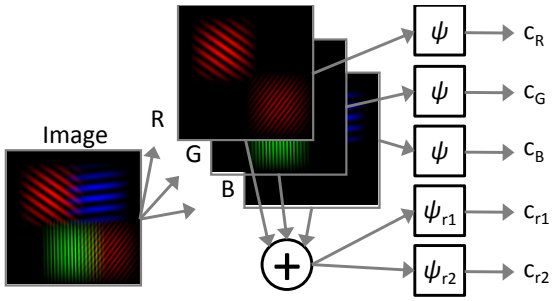

Figure 2: Color MWT scheme. Each color channel is analyzed with the primary wavelet transform symbolized by a ψ bloc and the sum "$R + G + B$" is analyzed with the "Riesz part" wavelet transform (ψ_{r1} and ψ_{r2} blocs).

4 COLOR MONOGENIC WAVELETS

We define here our proposition that combines a fundamental generalization of the monogenic signal to color with the monogenic wavelets described above. The challenge is to avoid the classical *marginal* definition that would be applying a *grayscale* monogenic transform on each of the three color channels of a color image. We believe that the monogenic signal has a favorable theoretical framework for a color extension and this is why we propose to start from this particular wavelet transform rather than from a more classical one.

The color generalization of the monogenic signal is expressed within the *geometric algebra* framework. This algebra is very general and embeds the complex and quaternion as subalgebras. Its elements are "multivectors" naturally linked with various geometric entities. The use of this fundamental tool is gaining popularity in the literature because it allows rewriting sophisticated concepts with simpler algebraic expressions and so paves the way to innovative ideas and generalizations in many fields.

For simplicity's sake and since anyway we would not have enough space to present the fundamentals of geometric algebra we here express the construction in classical terms; as we already did section 2. Yet we may sometimes point out some necessary specific mechanisms but we refer the reader to [4, 5] for further details.

4.1 The Color Monogenic Signal

Starting from Felsberg's approach that is originally expressed in the geometric algebra of $\mathbb{R}^3$; the extension proposed in [5] is written in the geometric algebra of $\mathbb{R}^5$ for 3-vector valued 2D signals of the form (s_R, s_G, s_B). By simply increasing the dimensions we can embed each color channel along a different axis and the original equation from Felsberg involving a 3D Laplace operator can be generalized in 5D with $\Delta_5 = \left(\frac{\delta}{\delta x_1} + \frac{\delta}{\delta x_2} + \frac{\delta}{\delta x_3} + \frac{\delta}{\delta x_4} + \frac{\delta}{\delta x_5}\right)$.

Then the system can be simplified by splitting it into three systems with a 3D Laplace equa-

tion, reducing to applying Felsberg's condition to each color channel. At this stage appears the importance of *geometric algebra* since an algebraic simplification between vectors leads to a 5-vector color monogenic signal that is non-marginal. Instead of naively applying the Riesz transform to each color channel, this fundamental generalization carries out the following color monogenic signal : $s_A = (s_R, s_G, s_B, s_{r1}, s_{r2})$ where s_{r1} and s_{r2} are the Riesz transform applied to $s_R + s_G + s_B$.

Now the color extension of Felsberg's monogenic signal is defined let us construct the color extension of the monogenic wavelets.

4.2 The Color Monogenic Wavelet Transform

We can now define a wavelet transform whose subbands are color monogenic signals. The goal is to obtain vector coefficients of the form $(c_R, c_G, c_B, c_{r1}, c_{r2})$ such that $c_{r1} = \frac{x}{2\pi\|\boldsymbol{x}\|^3} * (c_R + c_G + c_B)$ and $c_{r2} = \frac{y}{2\pi\|\boldsymbol{x}\|^3} * (c_R + c_G + c_B)$.

It turns out that we can very simply use the transforms presented above by applying the *primary* one on each color channel and the *Riesz part* on the sum of the three. The five related color wavelets illustrated Fig. 1 and forming one color monogenic wavelet ψ_A are :

$$\psi_R = \begin{pmatrix} \psi \\ 0 \\ 0 \end{pmatrix} \quad \psi_G = \begin{pmatrix} 0 \\ \psi \\ 0 \end{pmatrix} \quad \psi_B = \begin{pmatrix} 0 \\ 0 \\ \psi \end{pmatrix} \tag{7}$$

$$\psi_{r1} = \begin{pmatrix} \frac{x}{2\pi\|\boldsymbol{x}\|^3} * \psi \\ \frac{x}{2\pi\|\boldsymbol{x}\|^3} * \psi \\ \frac{x}{2\pi\|\boldsymbol{x}\|^3} * \psi \end{pmatrix} \quad \psi_{r2} = \begin{pmatrix} \frac{y}{2\pi\|\boldsymbol{x}\|^3} * \psi \\ \frac{y}{2\pi\|\boldsymbol{x}\|^3} * \psi \\ \frac{y}{2\pi\|\boldsymbol{x}\|^3} * \psi \end{pmatrix} \tag{8}$$

$$\psi_A = (\psi_R \ , \ \psi_G \ , \ \psi_B \ , \ \psi_{r1} \ , \ \psi_{r2}) \tag{9}$$

We then get 5-vector coefficients verifying our conditions and so forming a color monogenic wavelet transform. The associated decomposition is described by the diagram Fig. 2. This provides a multiresolution color monogenic analysis made of a 5-vector valued pyramid transform. The 5 decompositions of two images are shown Fig. 3 from left to right. Each one consists of 4 juxtaposed image-like subbands resulting from 3-level decomposition. We fixed $\gamma = 3$ that gave good experimental results.

Let us look at the first 3 graymaps. These are the 3 primary transforms c_R, c_G and c_B where white (resp. black) pixels are high positive (resp. negative) values. Note that our transform is non-separable and so provides at each scale only *one* subband related to *all* orientations. We are not subjected to the arbitrarily separated horizontal, vertical and diagonal analyses of usual wavelets. This advantage is even greater in color. Whereas marginal separable transforms show 3 arbitrary orientations within each color channel - which is not easily interpretable - the color monogenic wavelet transform provides a more compact *energy* representation of the color image content regardless of the local orientation. The color information is well separated through c_R, c_G and c_B : see that blue contours of first image are present only in c_B. And in each of the 3 decompositions it is clear that every orientation is equally represented all along the round contours. That is different from separable transform that privileges particular directions. The multiresolution framework makes the horizontal blue low frequency structure of second image be coded mainly in the third scale of c_B.

But the directional analysis is not lost thanks to the Riesz part that completes this representation. Now look at the "2-in-1" last decomposition forming the Riesz part. It is displayed in one

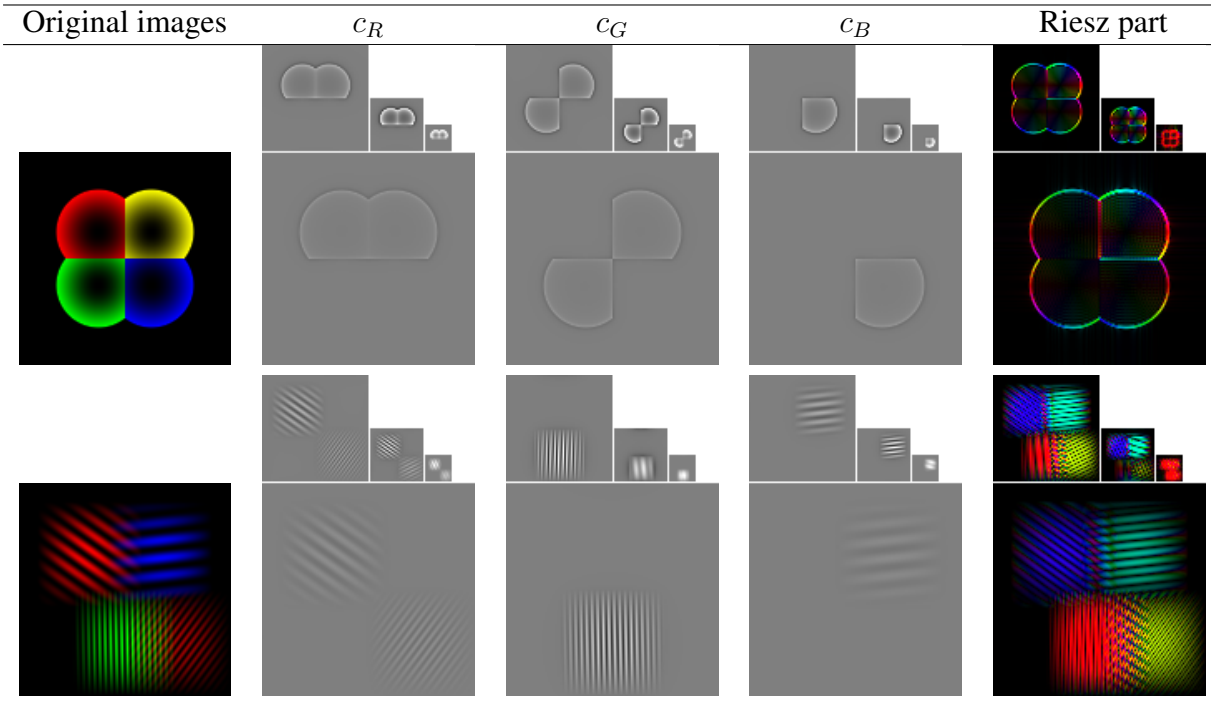

Figure 3: Color MWT of images. The two components of the *Riesz part* are displayed in the same graphic with the magnitude of $c_{r1}+\boldsymbol{j}c_{r2}$ encoded in the intensity and argument (local orientation) encoded in the hue.

color map where the geometric energy $\sqrt{c_{r1}^2+c_{r2}^2}$ is encoded into the intensity (with respect to the well known HSV color space) and the orientation $\arg\left(c_{r1}+\boldsymbol{j}c_{r2}\right)\,(\pi)$ is encoded in the hue (*e.g.* red is for $\{0,\pi\}$ and cyan is for $\pm\frac{\pi}{2}$). This way of displaying the Riesz part well reveals the provided geometric analysis of the image.

The Riesz part makes a precise analysis that is *local* both in space and scale. If there is a local color geometric structure in the image at a certain scale the Riesz part exhibits a high intensity in the corresponding position and subband. This is completed with an orientation analysis (hue) of the underlying structure. For instance a horizontal (resp. vertical) structure in the image will be coded by a cyan (resp. red) intense point in the corresponding subband. The orientation analysis is strikingly coherent and accurate. See for example that color structures with constant orientation (second image) exhibit a *constant* hue in the Riesz part over the whole structure.

Note that low intensity corresponds to "no structure" *i.e.* where the image has no geometric information. It is coherent not to display the orientation (low intensity makes the hue invisible) for these coefficients since this data has no sense in those cases.

In short the color and geometric information of the image are well separated from each other and the orientation analysis is very accurate. In addition the invariance properties of the primary and Riesz wavelet transforms are kept in the color extension for a slight overall redundancy of $20:9\approx 2.2$. This transform is non-marginal because RGB components is considered as well as intensity ($R+G+B$) - which involves two different color spaces.

5 WAVELET COEFFICIENTS STUDY FOR DENOISING ISSUE

Let us now study reduction of additive gaussian noise by wavelet domain thresholding. First we will experimentally characterize decomposition of a sole noise to identify effect of scale on

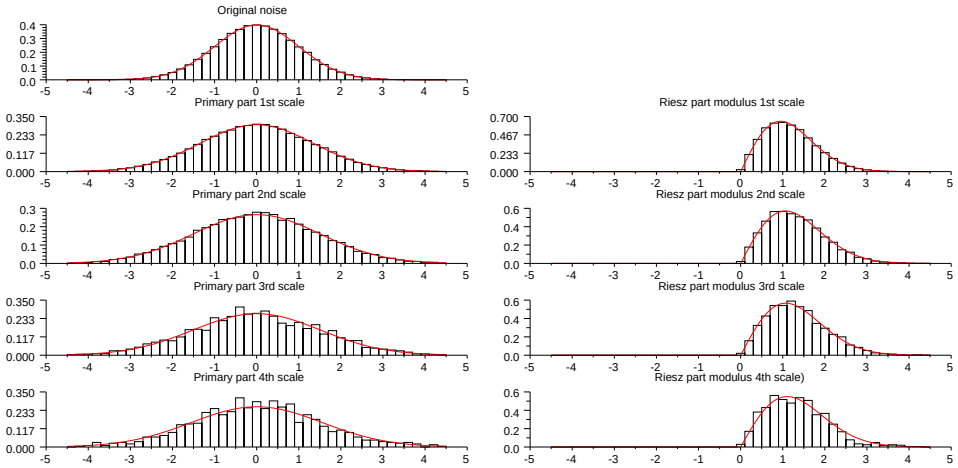

Figure 4: Histograms (bars) of primary subbands and modulus of Riesz subbands; and PDF models (line).

Scale s	1(High freq.)	2	3	4
St. dev. σ_s	1.339	1.502	1.512	1.560

Table 1: Standard deviations of subbands after decomposition of gaussian noise with variance 1 (with $\gamma = 3$).

distribution and subband correlation. Then we will apply color MWT thresholding to achieve color denoising and show experimental results.

5.1 Characterization of noise

With classical biorthogonal wavelets optimal thresholding involves a constant threshold over the whole transform (see
citeDonoho1995). Here we have a non-orthogonal transform so we need to study how the noise term of a noisy image is transformed through color monogenic wavelet analysis.

As shown Fig. 4 we observe that decomposition of a centered gaussian noise with variance σ^2 remains centered and gaussian after decomposition - with different variances though. For a given scale, distribution of Primary part as well as real and imaginary components of the Riesz part is clearly gaussian. Experimental values for standard deviations are given in table 1. These values can also be derived analytically from definition of filters. Recall that linear filtering of a stationary random signal x by filter H with output y can be studied with power spectral densities $\Psi_x = |\mathcal{F}[x]|^2$ (PSD) and autocorrelations $R_x(\tau) = \mathcal{F}^{-1}\Psi_x$. In particular we have $\Psi_y = \Psi_x|H|^2$. The output variance σ_y^2 is equal to $R_y(0)$ which reduces to $\sigma_y^2 = \frac{\sigma_x^2}{4\pi^2}\iint_{(0,0)}^{(2\pi,2\pi)} |H(\boldsymbol{\omega})|^2 \, d\boldsymbol{\omega}$.

For example the first scale output of our filterbank is directly linked to the first stage high-pass filter :

$$\sigma_1^2 = \frac{\sigma^2}{4\pi^2}\iint_{(0,0)}^{(2\pi,2\pi)} \left| \frac{\left(4(\sin^2\frac{\omega_1}{2} + \sin^2\frac{\omega_2}{2}) - \frac{8}{3}\sin^2\frac{\omega_1}{2}\sin^2\frac{\omega_2}{2}\right)^\gamma}{2\|\boldsymbol{\omega}\|^\gamma} \right|^2 d\boldsymbol{\omega} \qquad (10)$$

Remaining coefficients are tied to equivalent filters of each filterbank output.

A slight spatial correlation is introduced by the filterbank due to its redundancy. Whereas input noise autocorrelation $R = \sigma^2\delta$ is null for $\tau > 0$; R_s has some small coefficients around

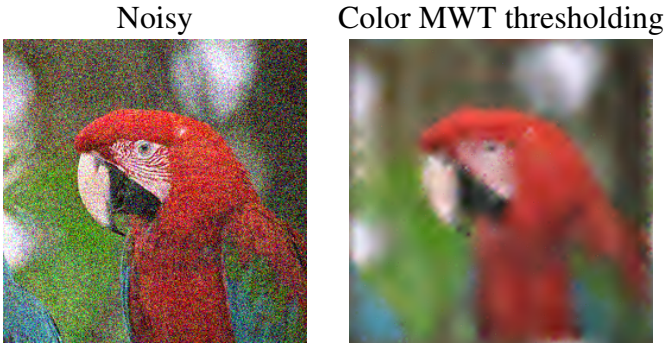

Figure 5: Denoising.

$\tau = 0$ - though with very fast decay - in a neighborhood of about 2 pixels (R_s is of the same form as wavelet functions showed Fig. 1). Some correlation is also present between primary and Riesz parts of subbands. So this transform has to be used carefully if some data compression is wanted.

Let us consider modulus of "Riesz part" outputs that will be of interest in the sequel. As real and imaginay part of subbands follow centered gaussian distributions with same variance σ_s^2, the complex subband follows a 2D isotropic gaussian distribution with variance $2\sigma_s^2$. As a result the modulus of "Riesz part" outputs follow a Rayleigh distribution $f_s(m) = \frac{m}{\sigma_s^2} e^{-m^2/2\sigma_s^2} \mathbf{1}_{m>0}$. We can see that modeled curves Fig. 4 well correspond to measured histograms.

Now that subbands are statistically modeled we can apply automatic thresholding to perform color denoising.

5.2 Thresholding

We apply a soft thresholding of color wavelet coefficients with a different threshold for each scale s. For the primary part threshold is fixed to $T_s^{prim} = k * \sigma_s$, with σ_s as reported in table 1 and $k = 3$. This choice of k is classical with usual wavelet denoising.

For the Riesz part that is complex valued we propose to threshold modulus because this data is tied to some *amplitude* information related to geometrical structures. But modulus follows a Rayleigh distribution so classical thresholding does not hold. A similar issue is dealt in [7] with modulus of gabor wavelets. Knowing that the mean (resp. variance) of a Rayleigh distribution is $\mu_r = \sigma\sqrt{\pi/2}$ (resp. $\sigma_r^2 = \sigma^2(4-\pi)/2$), the noise shrinkage threshold at each scale is set to be some number of standard deviations beyond the mean of the distribution - that is $\mu_r + k\sigma_r$. Since in our case a Rayleigh distribution is also involved this definition is pertinent for our Riesz part thresholding. So we have $T_s^{Riesz} = \sigma_s(\sqrt{\frac{\pi}{2}} + k\sqrt{\frac{4-\pi}{2}})$ (as in [7] we will take $k = 2$).

Threshold is classically estimated by a simple analysis of first scale (High frequencies) (see [8]). By assuming that first scale contains mainly noise plus a few significant coefficients, one can use the experimental median of coefficients to well estimate standard deviation of the gaussian noise distribution. So we have the estimate $\hat{\sigma} = \text{median}(|W_1|)/0.6745$ with W_1 being the coefficients of first scale. This estimation is done in the primary part but can be used for the Riesz part as both T_s^{prim} and T_s^{Riesz} only depends on estimate of σ_s. By using reference coefficients of Table 1 we use $\hat{\sigma_s} = \frac{\sigma_s}{\sigma_1}\hat{\sigma}$.

A result of color denoising is showed Fig. 5. This is a 4 scale thresholding of color MWT coefficients where T_s^{Prim} is used in Primary subbands and T_s^{Riesz} in the Riesz part. Thresholds

are processed from estimation of noise variance described above; and low frequency subband is not modified. This first result is comparable to a classical wavelet denoising and so confirms the potential of this transform. In practice the Riesz part remains difficult to deal with and many improvements may be added.

6 CONCLUSION

We define a color extension of the recent monogenic wavelet transform proposed in [3]. This extension is non-marginal since it takes care of considering a vector signal at the very beginning of the fundamental construction and leads to a definition basically different from the marginal approach. The use of non-separable wavelets joint with the monogenic framework allows for a good orientation analysis well separated from the color information. This color transform can be a great color image analysis tool thanks to this good separation of information through various data. A statistical modeling of coefficient for thresholding/denoising issue is given.

Although it is not marginal the color generalization has a marginal style since it reduces to apply the Riesz transform on the intensity of the image. So the geometric analysis is done without considering the color information and it would be much more attractive to have a complete representation of the color monogenic signal into magnitude and phase(s) with color/geometric interpretation.

REFERENCES

[1] I. W. Selesnick, R. G. Baraniuk, and N. G. Kingsbury, "The dual-tree complex wavelet transform," *IEEE Signal Processing Magazine [123] November*, 2005.

[2] W.L. Chan, H.H. Choi, and R.G. Baraniuk, "Coherent multiscale image processing using dual-tree quaternion wavelets," *IEEE Transactions on Image Processing*, vol. 17, no. 7, pp. 1069–1082, July 2008.

[3] M. Unser, D. Sage, and D. van de Ville, "Multiresolution monogenic signal analysis using the riesz-laplace wavelet transform," *IEEE Transactions on Image Processing*, vol. 18, no. 11, pp. 2402–2418, November 2009.

[4] M. Felsberg, "Low-level image processing with the structure multivector," *Thesis*, 2002.

[5] G. Demarcq, L. Mascarilla, and P. Courtellemont, "The color monogenic signal: a new framework for color image processing.," *IEEE Proceedings of the International Conference on Image Processing (ICIP)*, 2009.

[6] M. Unser and D. van de Ville, "The pairing of a wavelet basis with a mildly redundant analysis via subband regression," *IEEE Transactions on Image Processing*, vol. 17, no. 11, pp. 1–13, November 2008.

[7] P. Kovesi, "Phase preserving denoising of images," *The Australian Pattern Recognition Society Conference: DICTA99*, pp. 212–217, 1999.

[8] S. Mallat, *A wavelet tour of signal processing*, Academic Press, 1998.